Tsg101 positively regulates physiologic-like cardiac hypertrophy through FIP3-mediated endosomal recycling of IGF-1R

Kobina Essandoh,*,[1] Shan Deng,*,†,[1] Xiaohong Wang,* Min Jiang,‡ Xingjiang Mu,* Jiangtong Peng,†
Yutian Li,* Tianqing Peng,§ Kay-Uwe Wagner,¶ Jack Rubinstein,‡ and Guo-Chang Fan*,[2]

*Department of Pharmacology and Systems Physiology, University of Cincinnati College of Medicine, Cincinnati, Ohio, USA; †Department of Cardiology, Union Hospital–Tongji Medical College, Huazhong University of Science and Technology, Wuhan, China; ‡Division of Cardiovascular Health and Disease, Department of Internal Medicine, University of Cincinnati, Cincinnati, Ohio, USA; §Critical Illness Research, Lawson Health Research Institute, London, Ontario, Canada; and ¶Barbara Ann Karmanos Cancer Institute, Wayne State University School of Medicine, Detroit, Michigan, USA

ABSTRACT: Development of physiologic cardiac hypertrophy has primarily been ascribed to the IGF-1 and its receptor, IGF-1 receptor (IGF-1R), and subsequent activation of the protein kinase B (Akt) pathway. However, regulation of endosome-mediated recycling and degradation of IGF-1R during physiologic hypertrophy has not been investigated. In a physiologic hypertrophy model of treadmill-exercised mice, we observed that levels of tumor susceptibility gene 101 (Tsg101), a key member of the endosomal sorting complex required for transport, were dramatically elevated in the heart compared with sedentary controls. To determine the role of Tsg101 on physiologic hypertrophy, we generated a transgenic (TG) mouse model with cardiac-specific overexpression of Tsg101. These TG mice exhibited a physiologic-like cardiac hypertrophy phenotype at 8 wk evidenced by: *1*) the absence of cardiac fibrosis, *2*) significant improvement of cardiac function, and *3*) increased total and plasma membrane levels of IGF-1R and increased phosphorylation of Akt. Mechanistically, we identified that Tsg101 interacted with family-interacting protein 3 (FIP3) and IGF-1R, thereby stabilizing FIP3 and enhancing recycling of IGF-1R. *In vitro*, adenovirus-mediated overexpression of Tsg101 in neonatal rat cardiomyocytes resulted in cell hypertrophy, which was blocked by addition of monensin, an inhibitor of endosome-mediated recycling, and by small interfering RNA–mediated knockdown (KD) of FIP3. Furthermore, cardiac-specific KD of Tsg101 showed a significant reduction in levels of endosomal recycling compartment members (Rab11a and FIP3), IGF-1R, and Akt phosphorylation. Most interestingly, Tsg101-KD mice failed to develop cardiac hypertrophy after intense treadmill training. Taken together, our data identify Tsg101 as a novel positive regulator of physiologic cardiac hypertrophy through facilitating the FIP3-mediated endosomal recycling of IGF-1R.—Essandoh, K., Deng, S., Wang, X., Jiang, M., Mu, X., Peng, J., Li, Y., Peng, T., Wagner, K.-U., Rubinstein, J., Fan, G.-C. Tsg101 positively regulates physiologic-like cardiac hypertrophy through FIP3-mediated endosomal recycling of IGF-1R. FASEB J. 33, 7451–7466 (2019). www.fasebj.org

KEY WORDS: Rab11-FIP3 · exercise training · cardiac remodeling · membrane receptor · endosomes

Cardiac hypertrophy is an adaptive response to a variety of pathologic (*e.g.*, hypertension, myocardial infarction, and valve disease) and physiologic (*e.g.*, chronic exercise training) stress stimuli, which activate distinctive membrane receptors of cardiomyocytes and their downstream signaling pathways (1–3). It is generally accepted that the IGF-1, its cognate IGF-1 receptor (IGF-1R), and eventual activation of the protein kinase B (Akt) pathway

are involved in the development of physiologic cardiac hypertrophy (1–3). However, IGF-1–transgenic (TG) and IGF-1R–TG mice showed conflicting outcomes in relation to cardiac remodeling in mice (4, 5). For example, over-expression of IGF-1 in mouse hearts initially induced physiologic hypertrophy but ultimately progressed to a pathologic condition (*i.e.*, decreased systolic performance and increased interstitial fibrosis) (4). In contrast, mice with chronic overexpression of IGF-1R developed physiologic cardiac hypertrophy that was sustained into adulthood (5). Furthermore, ablation of cardiac IGF-1R postnatally in mice exhibited normal cardiac phenotype but blunted hypertrophic responses to exercise training (5). Hence, IGF-1R rather than IGF-1 is a critical regulator in the process of physiologic cardiac hypertrophy.

Like other receptor tyrosine kinases, total IGF-1R levels depend on either *de novo* synthesis or recycling and degradation through the cellular endosomal system. Upon stress or ligand stimulation, plasma membrane IGF-1R is dynamically altered by a series of endosome-associated steps, including endocytosis, sorting, recycling, and exocytosis (6–8). Usually, both ligand-occupied and unoccupied membrane receptors could be internalized by endocytosis to form early or sorting endosomes, which are targeted for transport by various endosome-associated Rab GTPases, such as Rab4a, Rab5a, Rab7, and Rab11a (9, 10). These Rab GTPases enable trafficking of sorting endosomes to various subcellular compartments, including late endosomes and lysosomes for degradation, the *trans*-Golgi network, and the endosomal recycling compartment (ERC) for recycling to the plasma membrane (9, 10). In glial cells, Romanelli *et al.* (11) observed that IGF-1R colocalized with Rab11 and the transferrin receptor, 2 classic ERC markers, suggesting that IGF-1R is targeted for recycling in response to continual ligand stimulation. These authors further showed that the recovery of IGF-1R at the cell surface by endosomal recycling is correlated with sustained Akt phosphorylation (11). Nonetheless, how to regulate endosome-mediated recycling of IGF-1R in cardiomyocytes during physiologic hypertrophy remains unknown.

Tumor susceptibility gene 101 (Tsg101) was initially defined as a negative regulator of tumorigenesis (12, 13). However, subsequent studies have described Tsg101 as a positive modulator of cancer progression, suggesting that Tsg101 may play divergent roles in carcinogenesis in different cell types (14–17). Actually, accumulating evidence now implicates Tsg101 as a versatile protein that has multiple cellular functions, including ubiquitination, transcriptional regulation, endosomal trafficking, virus budding, cytokinesis, cell survival, and proliferation (18). Importantly, as an integral member of the endosomal sorting complex required for transport machinery, Tsg101 has been shown to target ubiquitinated membrane receptors to late endosomes for lysosomal degradation (18). However, recent studies have also demonstrated that Tsg101 could target epidermal growth factor receptor (EGFR) to recycling endosomes and consequently induce positive effects on cellular homeostasis (19). Of interest, Horgan *et al.* (20) recently discovered that Tsg101 could bind to Rab11 family-interacting protein 3 (FIP3) in HeLa cells. FIP3 is an ERC protein that is critical for the structural integrity of the ERC (21–23). In conjunction with Rab11, FIP3 is actively involved in the endosomal-recycling processes of membrane proteins by coordinating delivery of endosomal cargo from early endosomes to the ERC (21–23). Given that IGF-1R is also distributed to the ERC, it would be intriguing to clarify whether Tsg101 regulates the process of endosome-mediated recycling of IGF-1R in cardiomyocytes.

In this study, cardiac Tsg101 was observed to be highly elevated in a physiologic hypertrophy model of treadmill-trained mice. We generated a TG mouse model with cardiac-specific overexpression of Tsg101, which showed enhanced recycling of IGF-1R and a physiologic hypertrophy–like phenotype with improved cardiac function without fibrosis. Similar results were achieved *in vitro*, where adenovirus-mediated overexpression of Tsg101 in neonatal rat cardiomyocytes (NRCMs) resulted in increased cell size. We also found that mice with cardiac-specific knockdown (KD) of Tsg101 were resistant to exercise-induced cardiac hypertrophy and showed decreased recycling of IGF-1R. Mechanistically, Tsg101 interacted with both IGF-1R and FIP3, possibly stabilizing and enhancing trafficking of IGF-1R to the ERC and to the plasma membrane.

MATERIALS AND METHODS

Animals

All mice used in this study were maintained and bred in the Division of Laboratory Animal Resources at the University of Cincinnati Medical Center. Animal experiments conformed to the *Guidelines for the Care and Use of Laboratory Animals* [National Institutes of Health (NIH), Bethesda, MD, USA] and approved by the University of Cincinnati Animal Care and Use Committee.

Physiologic hypertrophy model of treadmill exercise training

Male wild-type (WT) mice (7–8 wk of age) were acclimatized to the Omnipacer treadmill (Columbus Instruments, Columbus, OH, USA) for 3 d as follows: d 1, static treadmill for 5 min + 5 m/min for 5 min + 10 m/min for 5 min; d 2 and 3, 5 m/min for 5 min + 10 m/min for 5 min + 15 m/min for 5 min. Following acclimatization, mice underwent intense exercise training at 10 m/min for 5 min + an increase of 1 m/min every minute up to 25 m/min to induce cardiac hypertrophy. Mice were trained daily for 1 h or until mice were tired and unresponsive to shock stimuli for 10 s, as we previously described (24). Heart samples were collected after a 1-wk training period. Heart weight (HW) to body weight (BW) ratios were also measured.

Generation of Tsg101-TG mice

A 1.176-kb cDNA fragment of murine Tsg101 gene was cloned and inserted downstream of the cardiac-specific α-myosin heavy chain promoter (α-MHCp). This DNA vector was submitted to the Transgenic Animal and Genome Editing Core at Cincinnati Children's Hospital Center to generate a TG mouse model [Friend virus B NIH (FVB/N) background] with heart-specific overexpression of Tsg101. We performed routine genotyping by PCR with the use of an upper primer from the α-MHCp (5′-CACATAGAAGCCTAGCCCACAC-3′) and a lower primer from the Tsg101 DNA (5′-CCAATACAGGTTTGAGATC T-3′) to amplify a ~300-bp fragment spanning the junction between the α-MHCp and Tsg101 cDNA. The endogenous mouse thyroid–stimulating hormone-β gene was utilized as the internal

control with the forward primer 5′-TCCTCAAAGATGCTC-ATTAG-3′ and reverse primer 5′-GTAACTCACTCATGCAA-AGT-3′.

Isolation of cardiomyocytes and fibroblasts from mouse hearts

For cardiomyocyte isolation, the cannulated mouse heart was mounted on a Langendorff perfusion apparatus and perfused with Ca-free Tyrode solution (140 mM NaCl, 4 mM KCl, 1 mM MgCl2, 10 mMn glucose, and 5 mM HEPES, pH 7.4) at 37°C for 3 min. The perfusion buffer was replaced with the same solution containing liberase blendzyme I (0.25 mg/ml; Roche, Basel, Switzerland) and continued for 8–15 min until the heart became flaccid. The atria were removed, and the ventricular tissue was teased apart using Pasteur pipettes. The cell suspension was filtered through a 240-µm mesh screen, and the cardiomyocytes were allowed to settle by gravity for 15 min. Following sedimentation, Ca^{2+} was added sequentially at increasing concentrations to a final concentration of 1 mM. The final cardiomyocyte pellet was used for Western blot analysis.

For cardiac fibroblast isolation, the mouse heart was perfused and minced in HBSS. The minced tissue was digested in 0.2 mg/ml collagenase II (Worthington Biochemical, Lakewood, NJ, USA) and 0.25% trypsin at 37°C for 30 min. The digested tissue was then triturated 10 times and filtered through a 40-µm mesh. The resultant suspension was centrifuged for 5 min at 50 g at 4°C. The supernatant was transferred to a fresh tube and centrifuged at 500 g for 5 min. The fibroblast pellet was then suspended in DMEM [10% fetal bovine serum (FBS)] and cultured until the cells grew to full confluence.

Measurement of cardiac function and hypertrophy

Cardiac function and remodeling were determined by echocardiography with a Vevo 2100 Ultrasound System (Visualsonics, Toronto, ON, Canada) equipped with an MS400 probe (30-MHz centerline frequency) as previously described by Rubinstein et al. (25). Briefly, mice underwent anesthesia by isofluorane (1.5–2.0%). Parasternal long-axis and short-axis images were taken and analyzed with VevoStrain Software (Vevo 2100, v.1.1.1 B1455). Age- and weight-matched WT mice were used as controls. Ratios of HW:BW were measured as determinants of cardiac hypertrophy.

Cardiac histology

Mouse heart sections (5 µm in thickness) were produced from tissues and stained with Masson's Trichrome 2000 Kit (American MasterTech, Lodi, CA, USA) and PicroSirius Red Staining Kit (Thermo Fisher Scientific, Waltham, MA, USA) according to the manufacturers' protocols. To analyze individual cardiomyocyte size, heart sections were stained with wheat germ agglutinin (WGA) as we previously described (24). Images were taken under the microscope (Inteslight; Nikon, Tokyo, Japan), and the image-processing program ImageJ (NIH) was used to analyze cell sizes.

Isolation and culture of primary NRCMs

Rat neonates (2–3 d old) were anesthetized in an ice bath, and hearts were excised under sterile conditions. NRCMs were isolated using the Worthington Neonatal Cardiomyocytes Isolation System (Worthington Biochemical) according to the manufacturer's procedures. DMEM supplemented with 2% FBS and 1% antibiotics (penicillin and streptomycin) were used to culture NRCMs. NRCMs were treated with 20 ng/ml IGF-1 (Thermo Fisher Scientific) for 48 h as the *in vitro* model of physiologic hypertrophy.

Construction of adenovirus vector Tsg101 and transfection of cardiomyocytes

The adenovirus-expressing green fluorescent protein (GFP) (Ad.GFP)–fused Tsg101 (Ad.Tsg101) was generously offered by the lab of Dr. G. Paolo Dotto (Massachusetts General Hospital and Harvard Medical School, Boston, MA, USA). Plated NRCMs in dishes were infected with Ad.Tsg101 at 10 multiplicity of infection for 1 h. After 1-h transfection, cells were cultured in full DMEM (2% FBS and 1% antibiotics) for 48 h. The cells were collected for Western blotting assays after 48 h culture. NRCMs transfected with Ad.GFP were used as controls.

Western blotting assays

Total proteins were extracted from hearts or cultured myocytes, according to manufacturer's instructions, using the nonyl phenoxypolyethoxylethanol-40 (NP40) lysis buffer (Complete Mini; MilliporeSigma, Burlington, MA, USA) supplemented with protease inhibitor cocktail (Roche). Plasma membrane proteins were isolated using the Minute Plasma Membrane Protein Isolation Kit (Invent Biotechnologies, Plymouth, MN, USA) according to the manufacturer's protocol. Samples (10–100 µg) were subjected to SDS-PAGE as described in detail by Yang et al. (24). The dilutions and sources of the primary antibodies used in this study are as follows: rabbit anti–IGF-1R (1:1000; MilliporeSigma); mouse anti-Tsg101 (1:1000; Santa Cruz Biotechnology, Dallas, TX, USA); mouse anti-Akt (total Akt) (1:1000; Santa Cruz Biotechnology), rabbit anti–pAkt-Ser473 (1:1000; Santa Cruz Biotechnology); rabbit anti-FIP3 (1:500; Santa Cruz Biotechnology); rabbit anti–pAkt-Thr308 (1:500; Cell Signaling Technology, Danvers, MA, USA); rabbit anti-Rab7 (1:500; Cell Signaling Technology); rabbit anti-Rab4a (1:500; Proteintech, Rosemont, IL, USA); rabbit anti-Rab5a (1:500; Proteintech); rabbit anti-Rab11a (1:500; Proteintech); rabbit anti-periostin (1:500; Santa Cruz Biotechnology); and mouse anti–α-actin (1:1000; MilliporeSigma). Glyceraldehyde-3-phosphate dehydrogenase (GAPDH) (1:1000; Cell Signaling Technology) and sodium potassium ATPase (Na/K-ATPase) (1:1000; Cell Signaling Technology) were used as loading controls for total and plasma membrane protein levels, respectively. Western blot bands were quantified by MultiImage II (Proteinsimple, San Jose, CA, USA). The relative target protein levels were normalized to GAPDH for total protein and Na/K-ATPase for plasma membrane protein.

RT-PCR analysis

Total RNA from heart samples was isolated using the miRNeasy Mini Kit (Qiagen, Germantown, MD, USA). The quality and concentration of RNA was determined by the NanoDrop 2000 system (Thermo Fisher Scientific). The miScript PCR Starter Kit (Qiagen) was used to generate cDNA following the manufacturer's protocol. RT-PCR was performed in a total reaction volume of 20 µl using Sybr GreenER qPCR SuperMix (Thermo Fisher Scientific). Primer sets are listed in Supplemental Table S1. Relative fold expression for target genes was calculated by the $2^{-\Delta\Delta Ct}$ method.

Measurement of NRCM size

A total of 48 h after infection with Ad.GFP or Ad.Tsg101, NRCMs were washed twice with PBS and fixed with 4% paraformaldehyde for 10 min at room temperature. After fixing, NRCMs underwent permeabilization and blocking in PBS (5% bovine serum albumin, 0.3% Triton X-100) solution for 1 h at room temperature, after which cells were incubated with mouse anti–α-actinin antibody (1:500 dilution in PBS with 1% bovine

serum albumin; MilliporeSigma) at 4°C overnight. The next day, NRCMs were washed and stained with Alexa Fluor 594 goat anti-mouse IgG (1:500; Thermo Fisher Scientific) at room temperature for 1 h. Cells were imaged by confocal microscopy, and ImageJ was used to determine cell size.

Monensin treatment and small interfering RNA transfection

Monensin (MilliporeSigma) was dissolved in DMSO (Thermo Fisher Scientific) and then added to DMEM (without FBS) to a final concentration of 1 μM and then incubated in NRCMs for 1 h. Subsequently, cells were transfected with adenoviruses for 1 h and then cultured in full DMEM (2% FBS and 1% antibiotics) for a 48-h cell culture. Cells were collected after 48 h for Western blotting or fixed and stained with α-actinin antibody for measurement of the cell size, as described above. DMSO-pretreated NRCMs were used as control conditions. For small interfering RNA (siRNA) transfection, NRCMs were transfected with siRNA oligonucleotides targeting FIP3 (XM_001062633; MilliporeSigma) with the use of lipofectamine 200 (Thermo Fisher Scientific) as transfection agent for 72 h. Silencer Select Negative Control (4390843; Thermo Fisher Scientific) was transfected as control.

Coimmunoprecipitation assays

One milligram of mouse heart homogenate was solubilized in 1 ml of NP40 lysis buffer (with protease inhibitor cocktail) and precleared in 50 μl of protein A/G-agarose beads (Santa Cruz Biotechnology) for 1 h at 4°C on a rotary wheel. The mixture was then incubated with 1 μg of corresponding primary antibodies at 4°C overnight on a rotary wheel. Immunoprecipitates were collected and washed 5 times in NP40 lysis buffer. Immunoprecipitates were resolved in 2-times Laemmli sample buffer and boiled at 95°C for 5 min. Eluted proteins from the antibody-beads conjugate were subjected to SDS-PAGE.

Generation of cardiac-specific Tsg101-KD mice

The generation of mice having the floxed Tsg101 allele (Tsg101$^{fl/fl}$) under the 129/SvJ genetic background has been previously discussed by Wagner et al. (26). Genotyping primers were Tsg101^{fl}: forward 5′-AGAGGCTATTCGGCTATGACTG-3′, reverse 5′-TTCGTCCAGATCATCCTGATC-3′, Tsg101^{wt}: forward 5′-GTTCGCTGAAGTAGAGCAGCCAG-3′, reverse 5′-CATTTCTGGAGTCCGATGCGCAG-3′. Mice expressing an inducible Cre recombinase transgene driven by the α-MHCp were purchased from The Jackson Laboratory, Bar Harbor, ME, USA (005657). Tsg101$^{fl/fl}$ female mice were crossed with male mice expressing an inducible Cre recombinase transgene driven by the α-MHCp to obtain male heterozygotes (Tsg101$^{fl/wt}$: Cre positive), which were injected at 8 wk with tamoxifen (MilliporeSigma) to induce KD of Tsg101 in the heart. Tamoxifen was initially dissolved in ethanol and then in corn oil at 37°C to a stock concentration of 10 mg/ml. Mice were injected intraperitoneally at 1 mg/d for 5 consecutive d. Control (WT) mice were littermates that were either Tsg101$^{wt/wt}$ (Cre$^+$) or Tsg101$^{fl/wt}$ (Cre$^-$) but of the same genetic background. To induce physiologic hypertrophy in KD mice, mice were subjected to the exercise training as previously described for 4 wk.

Cell biotinylation-based recycling assays

Biotinylation recycling assay was conducted based on a procedure published previously by O'Reilly et al. (27) with few modifications. This assay relies on the principle that cell surface

proteins could be bound to membrane-impermeable biotin and then be internalized and subsequently recycled back at indicated incubation temperatures. The cell-impermeable reducing agent, sodium 2-mercaptoethanesulfonate (MESNA) is utilized to cleave recycled biotinylated proteins, and the resultant (i.e., intracellular) biotinylated IGF-1R are subjected to affinity purification with streptavidin beads and detection through immunoblot analysis. A total of 48 h after transfection of adenoviruses in NRCMs, cells were washed 3 times with cold PBS, 1 mM MgCl$_2$, and 0.1 mM CaCl$_2$ at 4°C. Cells were then incubated with 0.5 mg/ml sulfosuccinimidyl 2-(biotinamido)-ethyl-1,3-dithiopropionate (Thermo Fisher Scientific) at 4°C for 1 h. After 2 washes in PBS, 1 mM MgCl$_2$, 0.1 mM CaCl$_2$, and 25 mM glycine to neutralize free biotin, cells were treated with DMEM containing 20 ng and ml IGF-1 and returned to 37°C for 15 min to induce internalization and endocytosis of biotinylated receptors. Consequently, NRCMs were taken to 4°C and incubated with cell-impermeable (100 mM) MESNA in 50 mM Tris-Cl and 100 mM NaCl (pH 8.5) (MESNA buffer) to cleave off uninternalized biotinylated receptors. MESNA was quenched by 2 washes of 5 mg/ml iodoacetamide in PBS. Cells were then incubated in DMEM containing 20 ng/ml IGF-1 and returned to 37°C for 45 min to initiate recycling on internalized biotinylated receptors. Recycled biotinylated receptors were again cleaved with MESNA buffer, which was quenched in 5 mg/ml iodoacetamide. Cells were subsequently collected and subjected to streptavidin agarose (Thermo Fisher Scientific) in NP40 lysis buffer overnight. The next day, the streptavidin beads were washed 5 times in NP40 lysis buffer. The beads were resolved in 2-times Laemmli sample buffer and boiled at 70°C for 5 min. Eluted proteins from the streptavidin beads were subjected to SDS-PAGE and Western blotting for the detection of IGF-1R expression. For the immunofluorescence recycling assay, NRCMs were starved in serum-free medium for 4 h and then treated with 50 μg/ml cycloheximide for 1 h to prevent synthesis of new IGF-1R. At 4°C, cells were treated with IGF-1R antibody-biotin conjugate together with 20 ng/ml IGF-1. The preparation of the IGF-1R antibody-biotin conjugate was performed as previously described by Haugland et al. (28). The cells were then incubated at 37°C to allow internalization of IGF-1R biotin for 15 min. Cells were returned to 4°C, at which point uninternalized IGF-1R-biotin was cleaved with MESNA solution. Cells were then incubated in DMEM and 20 ng/ml IGF-1 at 37°C to induce recycling of internalized IGF-1R biotin for 45 min. Cells were subsequently fixed in 4% paraformaldehyde and incubated in Streptavidin Alexa Fluor 594 Conjugate (Thermo Fisher Scientific) at room temperature for 30 min to capture IGF-1R antibody biotin. Cells were visualized by confocal microscopy.

Statistical analysis

Data were expressed as means ± SD. Significance was determined by Student's t test and 1- or 2-way ANOVA to determine differences within groups where appropriate. A value of $P < 0.05$ was considered statistically significant.

RESULTS

Expression profiles of endosome-associated genes in treadmill-trained mouse hearts

The endosomal system plays a major role in the regulation of IGF-1R levels through endocytosis, recycling, and degradation (6–8). Rab GTPases, including Rab5a (regulates endocytosis and early endosome formation), Rab4a (mediates fast recycling of endosomes), Rab7 (promotes late endosome formation and fusion of endosomes with

lysosomes), and Rab11a (facilitates recycling of endosomes through the ERCs), are essential components of endosomal-related activities (9, 10) (**Fig. 1***A*). Other significant players include FIP3, which contributes to the structural integrity of the ERC, and Tsg101, which is a member of the endosomal sorting complex required for the endosomal transport (18, 21–23) (Fig. 1*A*). Given that IGF-1R is a critical regulator of physiologic hypertrophy, we sought to determine the expression profile of these endosomal-associated genes during physiologic cardiac hypertrophy. Mice (FVB/N background) were subjected to treadmill training for inducing physiologic cardiac hypertrophy, as we previously described (24). There was a significant increase in the ratio of HW:BW of treadmill-trained mice compared with sedentary control, confirming that the model was successfully generated (Fig. 1*B, C*).

Next, we observed that both total and plasma membrane levels of IGF-1R were higher in the hearts of exercised mice than sedentary controls (Fig. 1*D–F*), which is consistent with previous models of exercised-induced hypertrophy (2, 5, 11). Interestingly, protein levels of Rab5a, Rab7, and Rab11a were significantly elevated by 1.5-, 1.3-, and 1.9-fold, respectively, in exercise-trained mice compared with controls (Fig. 1*D, F*). These data suggest that endocytosis, recycling, and fusion of endosomes with lysosomes are enhanced in the myocardium during physiologic cardiac growth. However, cardiac levels of Rab4a were unchanged in treadmill-trained mice in relation to untrained controls (Fig. 1*D, F*). In a way similar to Rab11a, expression levels of FIP3 and Tsg101 were significantly increased by 1.4-fold and 3-fold, respectively, in treadmill-trained hearts (Fig. 1*D, F*), indicating that the Rab11a or FIP3-mediated endosomal recycling pathway is activated during the development of physiologic cardiac hypertrophy. In the same vein, treatment of NRCMs with IGF-1 resulted in increased cell size and significantly higher levels of Tsg101, FIP3, Rab5a, Rab11a, Rab7, Akt phosphorylation, and plasma membrane IGF-1R compared with vehicle-treated cells (Supplemental Fig. S1*A–C*). Taken together, these data suggest that the ERC-mediated endosomal recycling pathway is activated, which may be responsible for the recycling of IGF-1R in the heart during physiologic cardiac remodeling.

Generation and characterization of Tsg101-TG mouse model

Given that Rab11a and FIP3 are well known to regulate ERC-mediated endosomal recycling, whether Tsg101 also participates in such an endosomal recycling of IGF-1R in the heart has never been investigated. To this end, we generated a Tsg101-TG mouse model (FVB/N background) in which Tsg101 was overexpressed under the control of the cardiac-specific α-MHCp (**Fig. 2***A*). Western blotting analyses in heart samples showed that these TG lines overexpressed Tsg101 to 11-fold (line D) and 4-fold (line G) compared with WT hearts (Fig. 2*B, C*). Immunoblot analyses further demonstrated that Tsg101 was specifically overexpressed in cardiomyocytes but not in cardiac fibroblasts of TG mice (Supplemental Fig. S2*A, B*).
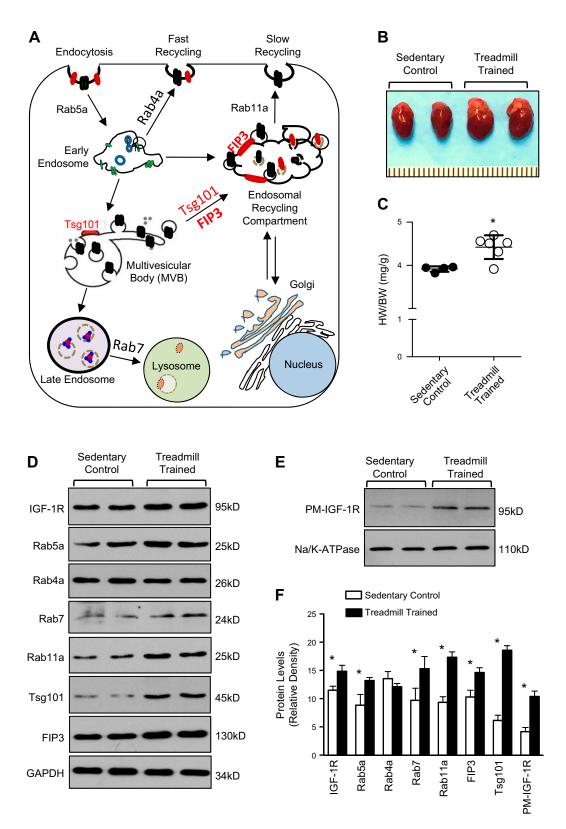
Next, we observed that both lines of TG mice exhibited features of physiologic cardiac hypertrophy but not pathologic remodeling based on the following results. First, TG hearts showed larger hearts compared with WTs (Fig. 2*D*), which was supported by significantly higher ratios of HW:BW in TGs than in WTs (Fig. 2*E*). Second, WGA staining of heart sections showed that the mean cardiomyocyte size was remarkably increased in Tsg101-TG mice by 3.1-fold (line D) and 2.1-fold (line G) compared with WTs (Fig. 2*D, F*). Third, TG hearts showed no signs of fibrosis after Masson Trichrome and Picrosirius Red staining of heart sections (Fig. 2*D*), which was further supported by RT-PCR demonstrating no changes in the expression of fibrosis markers, collagens I and III (Fig. 2*G*). Furthermore, we observed that cardiac function was enhanced in TG mice as evidenced by increased ejection fraction (17% in D; 24% in G) and fractional shortening (22% in D; 32% in G) in 2 TG lines compared with WTs (Fig. 2*H*). Put together, these results suggest that overexpression of Tsg101 could induce physiologic cardiac hypertrophy in mice.

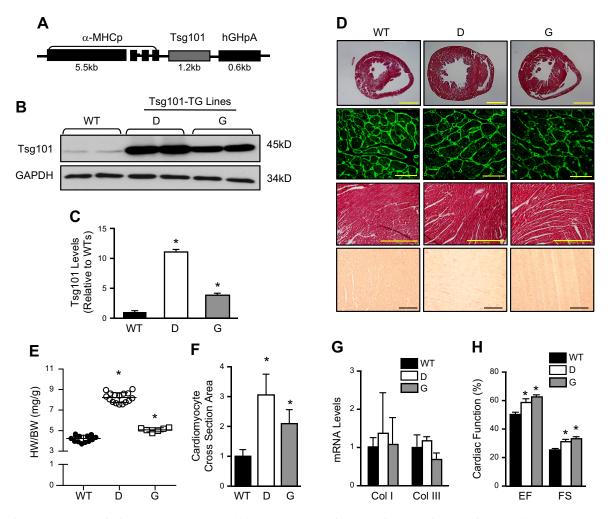## Overexpression of Tsg101 alters expression of endosome-associated proteins

Given that cardiac-specific overexpression of Tsg101 resulted in a phenotype similar to exercise-trained mice, we sought to investigate whether elevation of Tsg101 in the heart would have similar effects on the expression of endosome-associated genes. Western blot analyses showed that proteins levels of Rab5a and Rab7 were both significantly elevated in TG hearts compared with WTs, indicating that elevation of Tsg101 could promote endocytosis and maturation of the early to late endosome in the heart (**Fig. 3***A, B*). Rab4a, responsible for fast recycling of the early endosome, was unchanged in TG mice (Fig. 3*A, B*). Importantly, Rab11a and FIP3, 2 key members of the ERC, were greatly increased in TG hearts compared with WTs (Fig. 3*A, B*). Next, we sought to determine whether enhancement of recycling mediators would have any effects on IGF-1R levels and Akt signaling. As shown in Fig. 3*C, D*, both total and plasma membrane levels of IGF-1R were higher in TG hearts than in WTs ($n = 6$). Accordingly, the levels of phosphorylated Akt at sites of Thr308 and Ser473 were remarkably increased in TG lines compared with WTs (Fig. 3*C, D*). It is important to note that overexpression of Tsg101 in mouse hearts had no effect on mRNA levels of endosomal-associated genes (Supplemental Fig. S3*A, B*). Collectively, these data suggest that overexpression of Tsg101 enhances cardiac endosomal recycling of IGF-1R in a pattern similar to what we observed in treadmill-trained mouse hearts.

Overexpression of Tsg101 promotes IGF-1R recycling and cell growth in NRCMs

Considering that long-term overexpression of Tsg101 *in vivo* may have compensatory effects that may influence the phenotype of Tsg101 in the mouse heart, we next performed studies using *ex vivo* cultured NRCMs, a well-controlled

Figure 1. Exercise training elicits distinct expression of endosome-associated genes. *A*) Diagram showing structural components and major players involved in the endosomal system. *B, C*) Increased ratios of HW:BW in treadmill-trained mice compared with sedentary control mice; $n = 4$ for sedentary control mice, $n = 6$ for treadmill-trained mice. *D*) Western blots showing the differential expression of endosome-related genes in hearts of sedentary control and treadmill-trained mice. GAPDH was used as loading control. *E*) Western blots showing plasma membrane (PM) levels of IGF-1R in hearts of sedentary control and treadmill-trained mice. Na/K-ATPase was used as loading control. *F*) Quantitation of immunoblots (*D, E*); $n = 9$. *$P < 0.05$ *vs.* sedentary controls.

Figure 2. Generation and characterization of Tsg101-TG mice. *A*) Schematic diagram showing the Tsg101-TG construct. *B, C*) Western blots and quantification showing overexpression of Tsg101 in TG mouse hearts. GAPDH was used as loading control (*n* = 6). *D*) Histologic sections of hearts showed cardiac hypertrophy in TG lines compared with WT mice; *n* = 3 hearts for each group. Three constitutive sections of each heart were examined (scale bars, 5 mm). Immunostaining of heart sections from WT and TG lines with fluorescent-labeled WGA (Oregon Green 488–conjugated WGA, 1:500; scale bars, 20 μm). Representative images of Masson's Trichrome (scale bars, 200 μm) and Picrosirius Red staining (scale bars, 100 μm) showed no signs of histopathology. Three constitutive sections of each heart were stained. *E*) Increased ratios of HW:BW in Tsg101-TG mice compared with WT mice; *n* = 15 for WT, *n* = 17 for D, *n* = 7 for G. *F*) Quantification results for WGA staining of heart sections shown in *D*; *n* = 6. *G*) mRNA levels of cardiac fibrosis markers measured by RT-PCR; *n* = 5. *H*) Overexpression of Tsg101 improves cardiac function determined by echocardiography. Col I, collagen I; Col III, collagen III; D, transgenic line D; G, transgenic line G; *n* = 8 for WT, *n* = 6 for D, *n* = 7 for G. *$P < 0.05$ *vs.* WTs.

experimental setting. NRCMs were isolated from 2- to 3-d old neonatal rats and infected with Ad.Tsg101 or Ad.GFP for 48 h. Constructs for Ad.Tsg101 and control Ad.GFP are displayed in **Fig. 4*A***. Visually, Ad.Tsg101 cells were larger than Ad.GFP cells, and Tsg101 was distributed all over the cell as punctate structures (Fig. 4*B*). Western blotting analysis showed that Tsg101 was dramatically overexpressed in Ad.Tsg101-infected NRCMs compared with Ad.GFP cells (Note: the GFP-Tsg101 band was displayed around 82 kD) (Fig. 4*C*). The results of immunostaining with α-actinin antibody further affirmed the increased cell size by 2.3-fold in Ad.Tsg101 NRCMs compared with Ad.GFP cells (Fig. 4*D, E*). Most interestingly, Western blot assays revealed that both total and plasma membrane levels of IGF-1R were greatly increased in Ad.Tsg101 cells, accompanied by a remarkable elevation of phosphorylated Akt, in relation to Ad.GFP cells (Fig. 4*F, G*). As a matter of fact, the endosomal

recycling pathway was activated by the elevation of Tsg101, evidenced by higher levels of Rab5a, Rab7, Rab11, and FIP3 in Tsg101-infected cells, whereas Rab4a levels were unchanged compared with Ad.GFP cells (Fig. 4*F, G*). Similar to Tsg101-TG hearts, RT-PCR analyses showed that there were no changes in mRNA levels of endosome-associated genes in Ad.Tsg101 NRCMs in relation to controls (Supplemental Fig. S3*C, D*). Considering that plasma membrane levels of IGF-1R were elevated in Ad.Tsg101 NRCMs, we next sought to determine whether Tsg101 enhances recycling of IGF-1R by utilizing a cell biotinylation–based recycling assay. We observed that Ad.Tsg101-mediated overexpression of Tsg101 promoted larger proportion of internalized, biotinylated IGF-1R to be recycled back onto the cell surface compared with Ad.GFP cells (**Fig. 5**). Put together, these data indicate that overexpression of Tsg101 in NRCMs could activate the IGF-1R and Akt signaling

A

B

C

D

Figure 3. Elevation of Tsg101 in the heart augments endosomal recycling of IGF-1R. *A, B)* Representative Western blots (*A*) and quantification results (*B*) of protein levels of Rab5a, Rab4a, Rab7, Rab11a, and FIP3 in Tsg101-TG hearts compared with WTs. *C, D)* GAPDH was used as loading control. Representative Western blots (*C*) and quantification results (*D*) showing increased levels of total and plasma membrane IGF-1R and Akt phosphorylation in Tsg101-TG hearts compared with WTs. Total Akt was loading control for Akt phosphorylation, and Na/K-ATPase was loading control for plasma membrane protein. D, transgenic line D; G, transgenic line G; *n* = 6. *$P < 0.05$ *vs.* WTs.

pathway through increased availability of IGF-1R at the cell membrane, leading to cell hypertrophy.

Blockade of endosomal recycling by monensisn and KD of FIP3 dampens Tsg101-induced cell hypertrophy

To test whether Tsg101-induced hypertrophy is dependent on the endosome-mediated recycling of IGF-1R, we pretreated neonatal cardiomyocytes with monensin (1 μM), an inhibitor of endosome recycling (11). Monensin is a polyether antibiotic, known to target Na/H exchanger 6, that results in raised endosomal pH and disruptive transfer of proteins from recycling endosomes to cell membrane (29, 30). After 1 h pretreatment, neonatal cardiomyocytes were transfected with Ad.Tsg101 or Ad.GFP, followed by 48-h culture. Western blotting results revealed that endosomal-triggered recycling of IGF-1R was remarkably blocked by addition of monensin, as evidenced by reduced plasma membrane levels of IGF-1R in monensin-treated cells (**Fig. 6A, B**; *n* = 4). Consequently, immunofluorescence staining with α-actinin antibody showed that Tsg101-induced enlargement of neonatal cardiomyocytes was greatly suppressed by treatment with monensin (Fig. 6C, D).
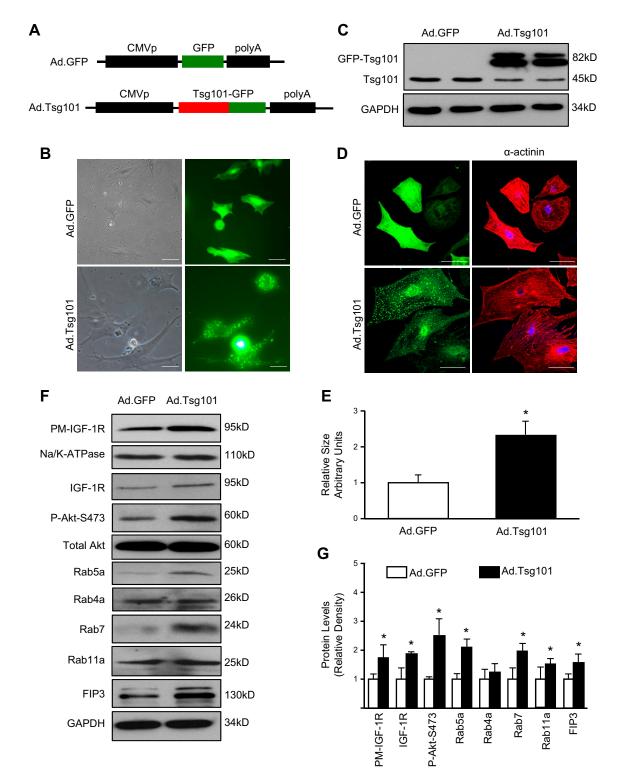
Considering that FIP3 is a critical contributor to endosomal-mediated recycling of receptors as part of the ERC (21), we sought to determine whether FIP3 is involved in Tsg101-induced hypertrophy. siRNA targeted at FIP3 (siFIP3) was employed to knock down FIP3 expression in neonatal cardiomyocytes. Transfection of siFIP3 resulted in successful down-regulation of FIP3 in Ad.GFP and Ad.Tsg101 NRCMs (Fig. 6E, F). Consequently, we observed that KD of FIP3 greatly blocked the Tsg101-induced cell hypertrophy (Fig. 6G, H). Hence, FIP3-

mediated endosomal recycling appears to be an essential for myocyte hypertrophy induced by overexpression of Tsg101.

Tsg101 interacts with FIP3 and IGF-1R in the heart

Tsg101 has recently been shown to interact with FIP3 in HeLa cells (20), but their interaction in cardiomyocytes remains unclear. To this end, we performed coimmunoprecipitation assays in the heart homogenates using antibodies to FIP3, Tsg101, or IGF-1R, respectively. Our results showed that not only did Tsg101 interact with FIP3 in WT hearts, but there was enhanced interaction in TGs (**Fig. 7A, B**). This suggests that Tsg101 binds to FIP3 at the ERC to propel recycling of endosomes. Furthermore, we observed that Tsg101 was also bound to IGF-1R (Fig. 7C, D), suggesting that Tsg101 may function as a bridge to recruit or connect IGF-1R to FIP3-containing recycling endosomes in the heart. To elucidate whether Tsg101, FIP3, and IGF-1R may exist in a complex, we performed coimmunofluorescence staining for FIP3 and IGF-1R in NRCMs transfected with Ad.Tsg101. Our results showed partial colocalization of Tsg101, FIP3, and IGF-1R (Fig. 7E), suggesting that Tsg101, FIP3, and IGF-1R might exist in a complex.
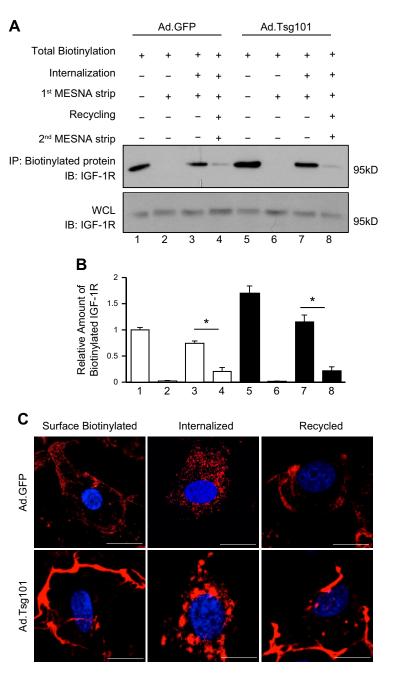
KD of Tsg101 inhibits development of physiologic cardiac hypertrophy

As presented above, overexpression of Tsg101 had positive effects on endosome-triggered recycling of IGF-1R and consequent activation of the Akt signaling, leading to physiologic cardiac growth. To determine whether Tsg101 is required during the process of physiologic cardiac

Figure 4. Overexpression of Tsg101 in NRCMs promotes cell hypertrophy. *A*) Diagrams depicting the recombinant adenoviral vectors Ad.GFP and Ad.Tsg101. *B*) Representative images showing Ad.GFP- or Ad.Tsg101-infected NRCMs (left panel is under bright field; right panel is the same field under fluorescence microscope). Scale bars, 20 μm. *C*) Western blot showing increased expression of Tsg101 in Ad.Tsg101 cardiomyocytes compared with Ad.GFP cells. *D, E*) Measurement of myocyte cross-sectional area in those infected cells (green) that were stained with cardiomyocyte-specific α-actinin antibody (red). Scale bars, 20 μm. *n* = 6 plates, 25–30 cells per plate. *F, G*) Representative immunoblots (*F*) and quantitative analyses (*G*) showing expression of PM IGF-1R, total IGF-1R, Akt phosphorylation at Ser473, Rab5a, Rab4a, Rab7, Rab11a, and FIP3 in Ad.Tsg101 and Ad.GFP cells. GAPDH was used as loading control for total protein, total Akt was loading control for Akt phosphorylation, and Na/K-ATPase was loading control for PM protein. PM, plasma membrane; *n* = 4 for independent experiments. *$P < 0.05$ *vs.* Ad.GFP cells.

A

	Ad.GFP				Ad.Tsg101			
Total Biotinylation	+	+	+	+	+	+	+	+
Internalization	−	−	+	+	−	−	+	+
1st MESNA strip	−	+	+	+	−	+	+	+
Recycling	−	−	−	+	−	−	−	+
2nd MESNA strip	−	−	−	+	−	−	−	+

IP: Biotinylated protein
IB: IGF-1R — 95kD

WCL
IB: IGF-1R — 95kD

1 2 3 4 5 6 7 8

B

Relative Amount of Biotinylated IGF-1R

C

	Surface Biotinylated	Internalized	Recycled
Ad.GFP			
Ad.Tsg101			

Figure 5. Overexpression of Tsg101 enhances recycling of IGF-1R in cardiomyocytes. *A, B*) Representative immunoblots (*A*) and quantitative analyses (*B*) of streptavidin immunoprecipitates (IP), visualized using an IGF-1R antibody. Whole-cell lysates (WCLs) were used as loading controls. Four independent experiments were performed for recycling assays. *C*) Representative images of immunofluorescence staining with streptavidin Alexa Fluor 594 conjugate after IGF-1R biotin was internalized and recycled in Ad.Tsg101 and Ad.GFP NRCMs; *n* = 4 plates, 25–30 cells per plate. Scale bars, 10 μm. *$P < 0.001$.

hypertrophy, we initially generated a mouse model with inducible cardiac-specific knockout of Tsg101 under the Cre and flox system. However, we observed that complete knockout of cardiac Tsg101 in adult mice was lethal within 1 wk after injection of tamoxifen. Indeed, prior work showed that global knockout of Tsg101 was lethal at the embryonic stage (27). Therefore, we generated an inducible, heart-specific, Tsg101-KD mouse model (129/SvJ background) (**Fig. 8***A*). Western blot analyses revealed that Tsg101 expression was down-regulated about 50% in such Tsg101-KD mouse hearts (Fig. 8*B*). Further analyses confirmed that reduction of Tsg101 protein levels in KD hearts is confined to cardiomyocytes rather than cardiac fibroblasts (Supplemental Fig. S4*A, B*). We next sought to determine the effects of Tsg101-KD on the endosome-mediated recycling of cardiac IGF-1R. As shown in Fig. 8*C, D*, protein levels of Rab11a and FIP3, 2 key components of recycling endosomes, were both significantly lower in Tsg101-KD hearts than in WTs, indicating suppressed activity of the endosomal recycling pathway. As a consequence, there were lower levels of total IGF-1R and plasma membrane IGF-1R in Tsg101-KD hearts than WTs (Fig. 8*C, D*). Notwithstanding, Tsg101-KD did not affect mRNA levels of Rab11a, FIP3, and IGF-1R (Supplemental Fig. S5*A*). Accordingly, Akt signaling was inhibited in Tsg101-KD hearts, as evidenced by reduced levels of Akt phosphorylation at sites of Thr308 and Ser473 compared with WTs (Fig. 8*C, D*).

To further determine the effect of Tsg101-KD on the development of exercise-induced physiologic cardiac

Figure 6. Tsg101-mediated cardiomyocyte hypertrophy is attenuated by monensin and KD of FIP3. *A, B*) Treatment of NRCMs with monensin (1 μM) 1 h prior to adenovirus infection resulted in reduced plasma membrane levels of IGF-1R; *n* = 4 for independent experiments; **P* < 0.05 *vs.* DMSO-pretreated GFP-cells, $^{\$}P$ < 0.05 *vs.* DMSO-pretreated control (Ctl) cells, $^{\&}P$ < 0.05 *vs.* DMSO-pretreated GFP cells, $^{\#}P$ < 0.05 *vs.* DMSO-pretreated Tsg101 cells. *C, D*) Representative images (*C*) of immunofluorescence staining with α-actinin and quantification (*D*) of cell cross-sectional area; *n* = 4 plates, 25–30 cells per plate. Scale bars, 20 μm. **P* < 0.05 *vs.* DMSO-pretreated GFP cells, $^{\#}P$ < 0.05 *vs.* DMSO-pretreated Tsg101 cells. *E, F*) Representative Western blots (*E*) and quantification (*F*) for Tsg101 and FIP3 protein levels in Ad.GFP and Ad.Tsg101 NRCMs transfected with control siRNA (siCtl) or siRNA targeted to FIP3 (siFIP3). GAPDH was loading control for total protein; *n* = 4 for independent experiments. **P* < 0.05 *vs.* Ad.GFP + siCtl, $^{\$}P$ < 0.05 *vs.* Ad.GFP + siCtl, $^{\&}P$ < 0.05 *vs.* Ad.Tsg101 + siCtl, $^{\#}P$ < 0.05 *vs.* Ad.GFP + siFIP3. *G, H*) Representative images (*G*) of immunofluorescence staining with α-actinin and quantification (*H*) of cell cross-sectional area; *n* = 4 plates, 25–30 cells per plate. Scale bars, 20 μm. **P* < 0.05 *vs.* Ad.GFP + siCtl, $^{\#}P$ < 0.05 *vs.* Ad.Tsg101 + siCtl.

hypertrophy, we subjected Tsg101-KD and WT mice to intense exercise training for 4 wk. In WT mice, there were significant increases in the HW:BW ratio and cardiomyocyte cross-sectional area after exercise training (Fig. 8*E–G*). However, Tsg101-KD mouse hearts failed to respond to exercise stimuli, as evidenced by no differences in HW:BW ratio and cardiomyocyte cross-sectional area compared with sedentary Tsg101-KD mice (Fig. 8*E–G*). Taken together, these results indicate that Tsg101 appears to be essential for the development of exercise-induced cardiac growth.
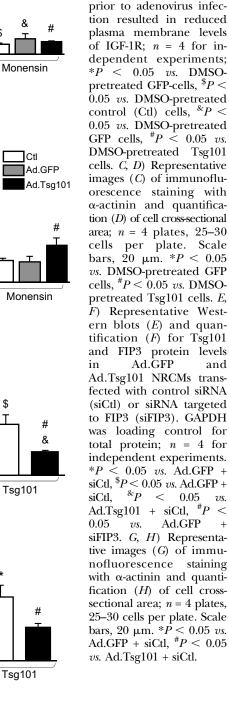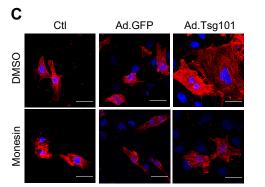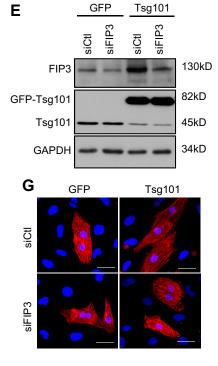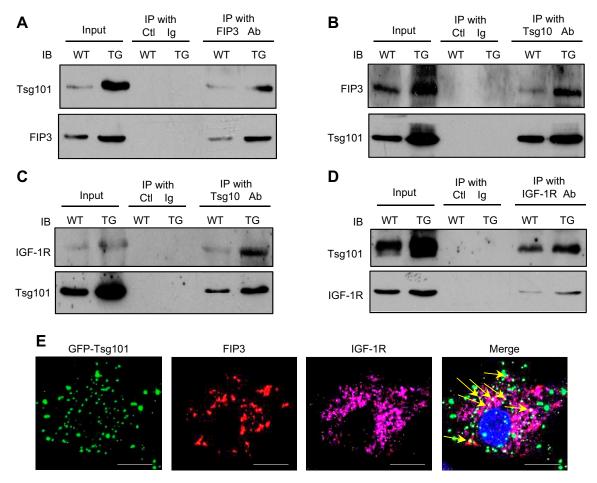
Figure 7. Tsg101 interacts with FIP3 and IGF-1R. *A, B*) Coimmunoprecipitations using anti-FIP3 (*A*) or anti-Tsg101 (*B*) as primary antibody, showing that the Tsg101 and FIP3 association was enhanced in TG (line G) hearts. *C, D*) Coimmunoprecipitations, using anti-Tsg101 (*C*) or anti–IGF-1R (*D*) as primary antibody, demonstrated that the Tsg101 and IGF-1R association was enhanced in TG (line G) hearts. WT and TG heart homogenates were used as input. *E*) Representative images showing partial colocalization for FIP3 and IGF-1R in Ad.Tsg101-infected NRCMs (yellow arrows). Similar results were observed in 3 additional, independent experiments. Ctl, control; IB, immunoblot; IP, immunoprecipitates. Scale bars, 20 μm.

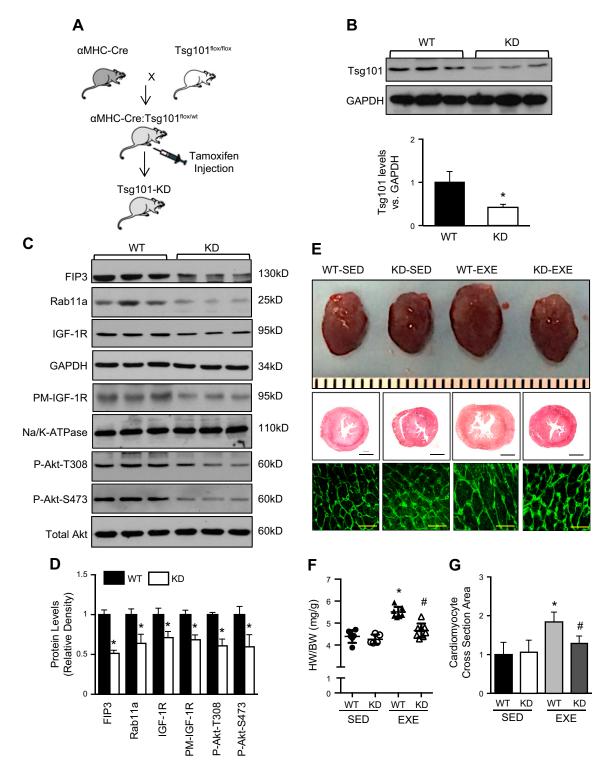## Tsg101 is required for recycling of IGF-1R

To further test the functional role of Tsg101 in the endosomal recycling of IGF-1R in cardiac myocytes, we utilized a cell surface biotinylation-based recycling assay in Tsg101-KD cardiomyocytes. Transfection of neonatal myocytes with adenovirus-expressing short hairpin RNA targeted to Tsg101 (Ad.shTsg101) resulted in about 75% reduction of Tsg101 levels (**Fig. 9A, B**). Protein levels, but not mRNA levels, of ERC members (Rab11a and FIP3) were reduced in Ad.shTsg101 NRCMs compared with adenovirus-expressing short hairpin RNA targeted to GFP (Ad.shGFP) cells (Fig. 9*A, B* and Supplemental Fig. S5*B*). Furthermore, total and plasma membrane levels of IGF-1R were diminished in Tsg101-KD myocytes, leading to reduced phosphorylation of Akt (Fig. 9*A, B*). In the recycling assay, KD of Tsg101 greatly impeded recycling of biotinylated IGF-1R, whereas a higher proportion of internalized biotinylated IGF-1R was recycled back to the plasma membrane in Ad.shGFP cells (Fig. 9*C, D*). In the immunofluorescence-based recycling assay, a large percentage of IGF-1R biotin fluorescent signals were observed at the cell periphery in Ad.shGFP NRCMs, whereas IGF-

1R biotin was visualized in intracellular sites in Ad.shTsg101 cells (Fig. 9*E*). Collectively, these data suggest that Tsg101 is required for the efficient recycling of IGF-1R in cardiomyocytes.
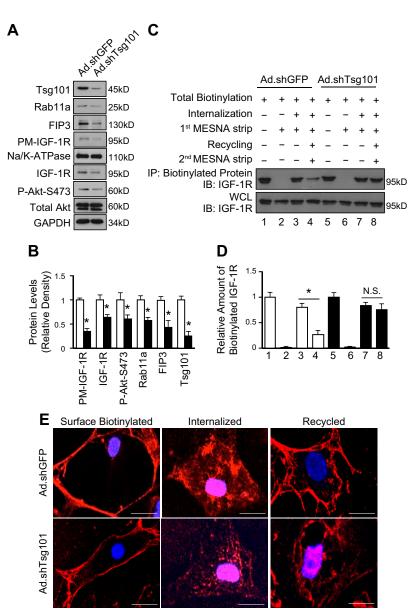
DISCUSSION

In this study, using both *in vivo* and *in vitro* gain- and loss-of-function approaches, we demonstrated that Tsg101 could be a critical mediator for the development of physiologic cardiac hypertrophy. Mechanistically, we identified that Tsg101 interacted with both FIP3 and IGF-1R in the heart, which may promote FIP3-triggered endosomal recycling of IGF-1R (**Fig. 10**), leading to physiologic cardiac growth.

IGF-1 and its cognate, IGF-1R, are pivotal to the exercise-induced cardiac hypertrophy (1–3). To provide balance between activation and inactivation of IGF-1 and IGF-1R signaling, IGF-1R is constitutively internalized into the cell to be recycled or degraded (6–8). Once internalized, the endosomal system regulates whether IGF-1R is degraded or recycled back to the plasma membrane (6–8).
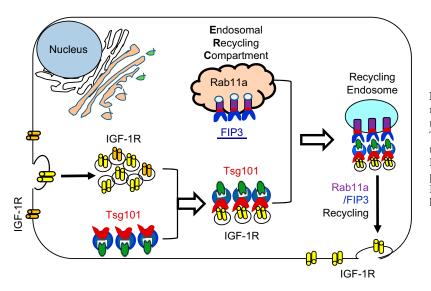
Figure 8. Cardiac-specific KD of Tsg101 inhibits development of exercise-induced cardiac hypertrophy. *A*) Schematic showing the generation of cardiac-specific Tsg101-KD mice. *B*) Representative Western blot and quantification results showing Tsg101 protein levels in Tsg101-KD hearts compared with WTs. GAPDH was used as loading control. *C, D*) Representative immunoblots (*C*) and quantitative analysis (*D*) showing protein levels of FIP3, Rab11a, total IGF-1R, plasma membrane (PM) IGF-1R, and Akt phosphorylation in Tsg101-KD and WT hearts. GAPDH was loading control for total protein, total Akt was loading control for Akt phosphorylation, and Na/K-ATPase was loading control for PM-IGF-1R. *E*) Whole hearts and histologic sections stained with fluorescent-labeled WGA (scale bars, 20 μm) in sedentary and treadmill-trained WT and KD mice. Three constitutive sections of each heart were stained. *F*) HW:BW measurements in sedentary and treadmill-trained WT and KD mice. *G*) Quantification results for WGA staining of heart sections shown in *E*. EXE, treadmill-trained mice; SED, sedentary mice; $n = 6$ hearts for all groups. *$P < 0.05$ *vs.* WT-SED, #$P < 0.05$ *vs.* WT-EXE.

Figure 9. KD of Tsg101 in neonatal myocytes blocks recycling of IGF-1R. *A, B*) Representative immunoblots (*A*) and quantitative analyses (*B*) showing protein levels of PM IGF-1R, total IGF-1R, Akt phosphorylation, Rab11a, FIP3, and Tsg101 in Ad.shTsg101 and Ad.shGFP NRCMs. GAPDH was loading control for total protein, total Akt was loading control for Akt phosphorylation, and Na/K-ATPase was loading control for PM; *n* = 4 for independent experiments; **P* < 0.05 *vs.* Ad.shGFP cells. *C, D*) Representative immunoblots (*C*) and quantitative analyses (*D*) of streptavidin IPs visualized using an IGF-1R antibody. WCLs were used as loading controls. Four independent experiments were performed for recycling assays. KD of Tsg101 inhibited recycling of IGF-1R, whereas recycling of IGF-1R was uninhibited in Ad.shGFP cells. *E*) Representative images of immunofluorescence staining with streptavidin Alexa Fluor 594 conjugate after IGF-1R biotin was internalized and recycled in Ad.shTsg101 and Ad.shGFP NRCMs. IP, immunoprecipitates; N.S., not significant; PM, plasma membrane protein; WCL, whole-cell lysate. *n* = 4 plates, 25–30 cells per plate. Scale bars, 5 μm. **P* < 0.001.

Nonetheless, whether and how the endosomal system regulates physiologic cardiac hypertrophy have not been studied thus far. In the present study, we did observe that major endosomal players were significantly up-regulated in the hearts of exercise-trained mice. Importantly, protein levels of Tsg101, a vital member of the endosomal system, were the most highly increased in exercise-trained mouse hearts, which compelled us to investigate its functional role in physiologic cardiac growth. Although Tsg101 was initially discovered as a tumor-associated protein, recent work has focused on the role of Tsg101 as part of the endosomal sorting machinery (18). Especially, recent studies had linked Tsg101 with trafficking of EGFR for degradation or recycling in tumor cells (31, 32). For example, Lu *et al.* (31) showed that the interaction of Tsg101 with the hepatocyte growth factor-regulated tyrosine kinase substrate, a component of endosomes, was critical for the recruitment of EGFR to late endosomes and to prevent its accumulation in early endosomes. Zhang *et al.* (32) observed that Tsg101 interacted with the biogenesis of lysosome-related organelles complex 1 and sorting

nexin 2 to mediate degradation of EGFR in lysosomal compartments. Moreover, Rush *et al.* (19) demonstrated that KD of Tsg101 impaired recycling of unliganded EGFR, causing accumulation of EGFR in low-density endosomes. Thus, besides sorting membrane proteins into endosomal compartments, Tsg101 seems to contribute to trafficking of membrane proteins for either degradation or recycling, leading to suppression or promotion of cancer cell growth. The present study identified that Tsg101 interacted with FIP3 in the heart, further supporting the notion that Tsg101 is recruited to ERCs. In addition, the interaction of Tsg101 with FIP3 and IGF-1R in the hearts may facilitate the stabilization of FIP3 and IGF-1R, leading to the elevation of their total protein levels in Tsg101-TG hearts. It is worth noting that the augmented interaction between Tsg101, FIP3, and IGF-1R in TG hearts may be due to increased protein levels of FIP3 and Tsg101. Consistent with our data presented here, Ismaili *et al.* (33) reported that Tsg101 could interact with and stabilize glucocorticoid receptor in HeLa cells, thereby preventing its degradation.

Figure 10. Diagram showing structural components and major players involved in the Tsg101-mediated endosomal recycling of IGF-1R. Tsg101 interacts with and enhances the function of FIP3 at the ERC. Increased activity of the ERC promotes translocation of IGF-1R to the plasma membrane, which in turn augments IGF-IR and Akt signaling in cardiac myocytes, leading to physiologic cardiac hypertrophy.

It is well known that downstream of IGF-1 and IGF-1R signaling is the Akt pathway, the most characterized pathway responsible for physiologic cardiac growth (5, 34–37). Currently, there are numerous regulators identified to target the Akt pathway or transcriptional control of gene programs associated with physiologic hypertrophy. For example, Boström *et al.* (38) reported that CCAAT-enhancer binding protein-β, a transcriptional factor, was down-regulated in swim-exercised mouse hearts. They found that reduction of CCAAT-enhancer binding protein-β triggered CREB-binding protein- and protein-300-interacting transactivator 4, which activated Akt and subsequent cardiomyocyte growth and proliferation (38). Recently, microRNAs have been shown to affect physiologic hypertrophy. For instance, we demonstrated that microRNA-233 could dysregulate a set of genes that lead to Akt activation and physiologic heart growth in mice (24). To date, regulation of physiologic cardiac growth through transcriptional factors or downstream control of Akt has been extensively studied. However, the role of the endosomal system in physiologic cardiac hypertrophy is uncertain. Thus, the present study, for the first time, defines Tsg101 as a novel regulator of physiologic cardiac hypertrophy through endosome-induced recycling of IGF-1R with the help of FIP3.

There are several limitations to this study. First, Tsg101-mediated recycling through the endosomal system may not be specific for IGF-1R. For example, Tsg101 has been shown to regulate recycling of the EGFR, which may contribute to the physiologic cardiac hypertrophy observed in this study. Nonetheless, in the present study, we mainly focused on whether the Tsg101-mediated endosomal recycling was involved in the turn-over of membrane IGF-1R, a key factor known to regulate physiologic cardiac growth. Second, this study did not decipher the possible role of Tsg101 in promoting endocytosis and late endosome and lysosome trafficking. Such analysis may fall outside the scope and intent of this report. Interestingly, we observed that Tsg101 positively regulated Rab7 expression in mouse hearts, which may stimulate the lysosomal degradation pathway. Indeed, lysosome-mediated degradation could provide new amino acids as building blocks for protein synthesis to assist the process of cardiomyocyte growth (39), therefore contributing to the Tsg101-induced physiologic cardiac hypertrophy.

In summary, our study elucidates a previously unrecognized role of Tsg101 in positively regulating physiologic cardiac hypertrophy. Specifically, elevation of cardiac Tsg101 is able to enhance FIP3 activity at ERCs, thereby stabilizing and driving IGF-1R recycling to promote activation of the Akt pathway, leading to physiologic cardiac growth in mice. This study may help us better understand the role of endosomal recycling in physiologic cardiac remodeling and therefore provide new strategies for the treatment of heart disease. Fj

AUTHOR CONTRIBUTIONS

K. Essandoh and S. Deng designed and performed experiments and analyzed data; X. Wang, X. Mu, J. Peng, and Y. Li performed experiments; M. Jiang and J. Rubinstein performed echocardiography analysis; T. Peng and K.-U. Wagner provided reagents and animals and reviewed and edited the manuscript; G.-C. Fan conceived and designed experiments and analyzed data; and G.-C. Fan is the guarantor of this work and, as such, had full access to all the data in this study and takes responsibility for the integrity of the data and the accuracy of the data analysis.

REFERENCES

1. Bernardo, B. C., Weeks, K. L., Pretorius, L., and McMullen, J. R. (2010) Molecular distinction between physiological and pathological cardiac hypertrophy: experimental findings and therapeutic strategies. *Pharmacol. Ther.* **128**, 191–227

2. Shimizu, I., and Minamino, T. (2016) Physiological and pathological cardiac hypertrophy. *J. Mol. Cell. Cardiol.* **97**, 245–262

3. McMullen, J. R., and Jennings, G. L. (2007) Differences between pathological and physiological cardiac hypertrophy: novel therapeutic strategies to treat heart failure. *Clin. Exp. Pharmacol. Physiol.* **34**, 255–262

4. Delaughter, M. C., Taffet, G. E., Fiorotto, M. L., Entman, M. L., and Schwartz, R. J. (1999) Local insulin-like growth factor I expression induces physiologic, then pathologic, cardiac hypertrophy in transgenic mice. *FASEB J.* **13**, 1923–1929

5. McMullen, J. R., Shioi, T., Huang, W.-Y., Zhang, L., Tarnavski, O., Bisping, E., Schinke, M., Kong, S., Sherwood, M. C., Brown, J., Riggi, L., Kang, P. M., and Izumo, S. (2004) The insulin-like growth factor 1 receptor induces physiological heart growth via the phosphoinositide 3-kinase (p110alpha) pathway. *J. Biol. Chem.* **279**, 4782–4793

6. Hicke, L. (1997) Ubiquitin-dependent internalization and down-regulation of plasma membrane proteins. *FASEB J.* **11**, 1215–1226

7. Hicke, L. (1999) Gettin' down with ubiquitin: turning off cell-surface receptors, transporters and channels. *Trends Cell Biol.* **9**, 107–112

8. Hicke, L. (2001) Protein regulation by monoubiquitin. *Nat. Rev. Mol. Cell Biol.* **2**, 195–201

9. Stenmark, H. (2009) Rab GTPases as coordinators of vesicle traffic. *Nat. Rev. Mol. Cell Biol.* **10**, 513–525

10. Bhuin, T., and Roy, J. K. (2014) Rab proteins: the key regulators of intracellular vesicle transport. *Exp. Cell Res.* **328**, 1–19

11. Romanelli, R. J., LeBeau, A. P., Fulmer, C. G., Lazzarino, D. A., Hochberg, A., and Wood, T. L. (2007) Insulin-like growth factor type-I receptor internalization and recycling mediate the sustained phosphorylation of Akt. *J. Biol. Chem.* **282**, 22513–22524

12. Li, L., and Cohen, S. N. (1996) Tsg101: a novel tumor susceptibility gene isolated by controlled homozygous functional knockout of allelic loci in mammalian cells. *Cell* **85**, 319–329

13. Moberg, K. H., Schelble, S., Burdick, S. K., and Hariharan, I. K. (2005) Mutations in erupted, the Drosophila ortholog of mammalian tumor susceptibility gene 101, elicit non-cell-autonomous overgrowth. *Dev. Cell* **9**, 699–710

14. Zhu, G., Gilchrist, R., Borley, N., Chng, H. W., Morgan, M., Marshall, J. F., Camplejohn, R. S., Muir, G. H., and Hart, I. R. (2004) Reduction of TSG101 protein has a negative impact on tumor cell growth. *Int. J. Cancer* **109**, 541–547

15. Carstens, M. J., Krempler, A., Triplett, A. A., Van Lohuizen, M., and Wagner, K. U. (2004) Cell cycle arrest and cell death are controlled by p53-dependent and p53-independent mechanisms in Tsg101-deficient cells. *J. Biol. Chem.* **279**, 35984–35994

16. Ruland, J., Sirard, C., Elia, A., MacPherson, D., Wakeham, A., Li, L., de la Pompa, J. L., Cohen, S. N., and Mak, T. W. (2001) p53 accumulation, defective cell proliferation, and early embryonic lethality in mice lacking tsg101. *Proc. Natl. Acad. Sci. USA* **98**, 1859–1864

17. Krempler, A., Henry, M. D., Triplett, A. A., and Wagner, K. U. (2002) Targeted deletion of the Tsg101 gene results in cell cycle arrest at G1/S and p53-independent cell death. *J. Biol. Chem.* **277**, 43216–43223

18. Slagsvold, T., Pattni, K., Malerød, L., and Stenmark, H. (2006) Endosomal and non-endosomal functions of ESCRT proteins. *Trends Cell Biol.* **16**, 317–326

19. Rush, J. S., and Ceresa, B. P. (2013) RAB7 and TSG101 are required for the constitutive recycling of unliganded EGFRs via distinct mechanisms. *Mol. Cell. Endocrinol.* **381**, 188–197

20. Horgan, C. P., Hanscom, S. R., Kelly, E. E., and McCaffrey, M. W. (2012) Tumor susceptibility gene 101 (TSG101) is a novel binding-partner for the class II Rab11-FIPs. *PLoS One* **7**, e32030

21. Horgan, C. P., Oleksy, A., Zhdanov, A. V., Lall, P. Y., White, I. J., Khan, A. R., Futter, C. E., McCaffrey, J. G., and McCaffrey, M. W. (2007) Rab11-FIP3 is critical for the structural integrity of the endosomal recycling compartment. *Traffic* **8**, 414–430

22. Junutula, J. R., Schonteich, E., Wilson, G. M., Peden, A. A., Scheller, R. H., and Prekeris, R. (2004) Molecular characterization of Rab11 interactions with members of the family of Rab11-interacting proteins. *J. Biol. Chem.* **279**, 33430–33435

23. Horgan, C. P., Hanscom, S. R., Jolly, R. S., Futter, C. E., and McCaffrey, M. W. (2010) Rab11-FIP3 links the Rab11 GTPase and cytoplasmic dynein to mediate transport to the endosomal-recycling compartment. *J. Cell Sci.* **123**, 181–191

24. Yang, L., Li, Y., Wang, X., Mu, X., Qin, D., Huang, W., Alshahrani, S., Nieman, M., Peng, J., Essandoh, K., Peng, T., Wang, Y., Lorenz, J., Soleimani, M., Zhao, Z. Q., and Fan, G. C. (2016) Overexpression of miR-223 tips the balance of pro- and anti-hypertrophic signaling cascades toward physiologic cardiac hypertrophy. *J. Biol. Chem.* **291**, 15700–15713

25. Rubinstein, J., Lasko, V. M., Koch, S. E., Singh, V. P., Carreira, V., Robbins, N., Patel, A. R., Jiang, M., Bidwell, P., Kranias, E. G., Jones, W. K., and Lorenz, J. N. (2014) Novel role of transient receptor potential vanilloid 2 in the regulation of cardiac performance. *Am. J. Physiol. Heart Circ. Physiol.* **306**, H574–H584

26. Wagner, K. U., Krempler, A., Qi, Y., Park, K., Henry, M. D., Triplett, A. A., Riedlinger, G., Rucker III, E. B., and Hennighausen, L. (2003) Tsg101 is essential for cell growth, proliferation, and cell survival of embryonic and adult tissues. *Mol. Cell. Biol.* **23**, 150–162

27. O'Reilly, M. K., Tian, H., and Paulson, J. C. (2011) CD22 is a recycling receptor that can shuttle cargo between the cell surface and endosomal compartments of B cells. *J. Immunol.* **186**, 1554–1563

28. Haugland, R. P., and Bhalgat, M. K. (2008) Preparation of avidin conjugates. *Methods Mol. Biol.* **418**, 1–12

29. Yamashiro, D. J., and Maxfield, F. R. (1984) Acidification of endocytic compartments and the intracellular pathways of ligands and receptors. *J. Cell. Biochem.* **26**, 231–246

30. Prasad, H., and Rao, R. (2015) The Na+/H+ exchanger NHE6 modulates endosomal pH to control processing of amyloid precursor protein in a cell culture model of Alzheimer disease. *J. Biol. Chem.* **290**, 5311–5327

31. Lu, Q., Hope, L. W., Brasch, M., Reinhard, C., and Cohen, S. N. (2003) TSG101 interaction with HRS mediates endosomal trafficking and receptor down-regulation. *Proc. Natl. Acad. Sci. USA* **100**, 7626–7631

32. Zhang, A., He, X., Zhang, L., Yang, L., Woodman, P., and Li, W. (2014) Biogenesis of lysosome-related organelles complex-1 subunit 1 (BLOS1) interacts with sorting nexin 2 and the endosomal sorting complex required for transport-I (ESCRT-I) component TSG101 to mediate the sorting of epidermal growth factor receptor into endosomal compartments. *J. Biol. Chem.* **289**, 29180–29194

33. Ismaili, N., Blind, R., and Garabedian, M. J. (2005) Stabilization of the unliganded glucocorticoid receptor by TSG101. *J. Biol. Chem.* **280**, 11120–11126

34. Condorelli, G., Drusco, A., Stassi, G., Bellacosa, A., Roncarati, R., Iaccarino, G., Russo, M. A., Gu, Y., Dalton, N., Chung, C., Latronico, M. V. G., Napoli, C., Sadoshima, J., Croce, C. M., and Ross, J., Jr. (2002) Akt induces enhanced myocardial contractility and cell size in vivo in transgenic mice. *Proc. Natl. Acad. Sci. USA* **99**, 12333–12338

35. Matsui, T., Li, L., Wu, J. C., Cook, S. A., Nagoshi, T., Picard, M. H., Liao, R., and Rosenzweig, A. (2002) Phenotypic spectrum caused by transgenic overexpression of activated Akt in the heart. *J. Biol. Chem.* **277**, 22896–22901

36. Cho, H., Thorvaldsen, J. L., Chu, Q., Feng, F., and Birnbaum, M. J. (2001) Akt1/PKBalpha is required for normal growth but dispensable for maintenance of glucose homeostasis in mice. *J. Biol. Chem.* **276**, 38349–38352

37. DeBosch, B., Treskov, I., Lupu, T. S., Weinheimer, C., Kovacs, A., Courtois, M., and Muslin, A. J. (2006) Akt1 is required for physiological cardiac growth. *Circulation* **113**, 2097–2104

38. Boström, P., Mann, N., Wu, J., Quintero, P. A., Plovie, E. R., Panáková, D., Gupta, R. K., Xiao, C., MacRae, C. A., Rosenzweig, A., and Spiegelman, B. M. (2010) C/EBPβ controls exercise-induced cardiac growth and protects against pathological cardiac remodeling. *Cell* **143**, 1072–1083

39. Dorn II, G. W. (2007) The fuzzy logic of physiological cardiac hypertrophy. *Hypertension* **49**, 962–970